

Electrochemical Synthesis of Nanostructured Oxide Layers on Threaded Surfaces of Medical Implants

OCTAV MARIUS RUSSU^{1*}, GABRIELA STRNAD^{2*}, LASZLO JAKAB-FARKAS³, RAZVAN CAZACU², ANDREI FEIER¹, ISTVAN GERGELY¹, CRISTIAN TRAMBITAS¹, CECILIA PETROVAN⁴

¹University of Medicine and Pharmacy, Faculty of Medicine, 38 Gh. Marinescu, 540139, Tirgu Mures, Romania

²Petru Maior University of Tirgu Mures, Faculty of Engineering, 1 Nicolae Iorga Str., 540088, Tirgu Mures, Romania

³Sapientia University of Cluj Napoca, Faculty of Technical and Human Sciences, 1C Sighisoarei, 540485, Tirgu Mures, Romania

⁴University of Medicine and Pharmacy, Faculty of Dental Medicine, 38 Gh. Marinescu, 540139, Tirgu Mures, Romania

Self organized nanostructured oxide layers were developed on threaded surfaces of medical implants made of Ti6Al4V alloy. The synthesis was done by electrochemical anodization in phosphate/fluoride based electrolyte. By anodization in an aqueous solution of 9.34 wt.% H_3PO_4 and 0.4 wt.% HF the threaded surfaces were covered by continuous, self ordered nanoporous oxide layers. Scanning electron microscopy (SEM) was used to evaluate the morphology of the nanostructured layers. The diameters of the nanopores depends on anodization potential, by using $U = 24$ V the openings had an average diameter of 40 nm, while using $U = 30$ V the average nanopores diameter was of 63 nm. The current density was ~ 10 A/m² in the steady state of potentiodynamic stage of anodization, and below 45 A/m² in potentiostatic stage.

Keywords: nanoporous TiO₂, nanotubes, electrochemical anodization, medical implants

Nanoporous and nanotubular TiO₂ (titania) structures are currently under intense research focus and have applications in photovoltaic cells, catalysis, biosensing, drug delivery, and medical implants. The most used materials for medical implants are titanium and its alloys, especially Ti6Al4V alloy. These materials are easily passivated by natural formation of a native compact oxide layer of 2-10 nm thickness on their surface. The presence of an oxide layer, in particular with a developed surface, enhances implants biocompatibility and osseointegration. Thus, surface modification at nanoscale level, by synthesis of nanoporous/nanotubular oxide layer have gained much attention in the recent years, many in vitro and in vivo studies showing that ordered nanostructures with openings of 15-100 nm combine very well with osseous tissue being the perfect basis for the osteoblasts integration during the process of bone regeneration and are well suited for bone implant industry [1-10].

Electrochemical anodization (EA) is a cost-effective method that permits the synthesis of nanostructured oxide layers when process parameters (electrolyte, current parameters, prior surface preparation, distance anode-cathode, duration) are optimized, allowing a proper control on morphology, structure, and chemical composition of oxide layers [11-17]. The growth mechanism of nanopores/nanotubes is complex and involves equilibrium condition between the formation of the oxide at the metal-oxide interface and its dissolution at the oxide-electrolyte interface. The presence of fluoride ions in the electrolyte is of extreme importance, creating the conditions for titanium material solvatization as soluble fluoride complexes [TiF₆]²⁻ and for nanopores/nanotubes growth. In the absence of fluoride ions the oxide layer which is developing is a compact one. By EA in fluoride based solutions the structure of oxide layer is amorphous.

Studies on EA optimization for the synthesis of adherent and ordered oxide layers onto the titanium based material substrate mainly considered planar surfaces in the form of flat foil. But the medical implants, for example dental

implants, or orthopedic implants for fracture fixation (screw, plates) or joint replacement present various shapes, cylindrical, conical, and threaded, and complex geometries with curves, edges and grooves. On this kind of complex substrates, the electrochemical anodization to produce uniform, highly ordered nanoporous/nanotubular oxide structures remains challenging, in the literature being very few studies focused on this issue [18-21].

The aim of present paper is to develop uniform, ordered nanostructured (nanoporous or nanotubular) oxide layer, by using electrochemical anodization in phosphate/fluoride electrolyte, on threaded surfaces of dental implants.

Experimental part

The present set of experiments was made on commercial MIS M4 implants (MIS Implants Technologies), internal hexagon type, with 4.2 mm diameter and 13 mm length, made of Ti6Al4V ELI titanium alloy, specimens designated as NS01-THR and NS02-THR. The external threaded surface of the implants, with an initial micro rough topography, was modified by electrochemical anodization in order to achieve its modification at nanoscale level. For comparison purposes, planar and cylindrical surfaces were modified using the same process parameters of anodization. Planar sample (ϕ 16 x 3 mm disc shape) designated as NS03-PLA, and cylindrical sample (ϕ 3.8 x 20 mm cylinder shape) designated as NS04-CYL, were made by Ti6Al4V titanium alloy. The initial planar and cylindrical surfaces were processed by turning on Cincom K16 (Citizen) CNC turning machine, followed by wet grinding with 320-grit and 1200-grit papers (ATM) done for 5 minutes. The resulting roughness of the surfaces, measured on SJ-310 (Mitutoyo) roughness tester, was of $R_a \sim 0.5$ μ m, corresponding to micro rough topographies of commercially available medical implants.

Before electrochemical anodization the samples were cleaned in a three-step procedure: ultrasonic cleaning in deionized water by using 3.0 Dr. Mayer ultrasonic cleaning machine (Dr. Mayer Life & Health) for 5 min, cleaning in

* email: russuo@yahoo.com; gabriela.strnad@ing.upm.ro

ethyl alcohol, and drying at 80°C for 20 minutes in BOV-T25F (Biobase) drying unit.

Electrochemical anodization was done in a custom built electrochemical set-up with two electrode configuration (fig. 1), designed and realized by us. The sample was connected to the anode, the cathode was a planar foil of pure copper, and the distance anode-cathode was 15 mm. The electrolyte was a solution of 9.34 wt.% phosphoric acid and 0.4 wt.% hydrofluoric acid, prepared from reagent grade chemicals (Chemical Company) and deionized water. The programmable dual range DC power supply 9184B (BK Precision) provided the anodization potential and APPA 505 (APPA Technologies) digital multimeter monitored the evolution of current during the anodization. The end potential was 24 V, or 30 V, applied with an initial potential ramp of 0.08 V/S. After the end potential was reached, the holding time for potentiostatic stage of the anodization was 30 min. The process parameters were controlled by our originally designed and realized software - Nanosource 2- that also allows the real time visualization and registration of process data. After anodization the samples were rinsed with deionized water, cleaned in ethyl alcohol and dried in air.

Surfaces morphology was examined by scanning electron microscopy (SEM) by using JSM 5200 (JEOL) scanning electron microscope, operated at 25 kV. The micrographs were collected at 35X, 1500X, 10000X, 20000X, and 35000X magnifications. The dimensions of nanostructures developed on modified surfaces were measured on SEM micrographs using Gimp 2.8.14 open source graphical image processing software. On each micrograph 50 nanostructures were selected and their features were measured, the results presented in the paper being the average values of these measurements.

Results and discussions

The material of the specimens - Ti6Al4V - is a two phase ($\alpha+\beta$) titanium alloy, where hexagonal closed packed (hcp) α phase is stabilized by 5.5-6.5% content of

aluminium, and body centred cubic (bcc) β phase is stabilized by 3.5-4.5% content of vanadium. The alloy exhibits very good mechanical properties: high tensile strength (860 MPa), low elastic modulus (114 GPa), and excellent fatigue strength (>1000000 cycles at 600 MPa). Its high biocompatibility is due to the fact that the outer surface of the material is naturally covered with a thin layer (2-10 nm) of TiO₂, titanium oxide.

MIS M4 ϕ 4.2 x 13 mm implants that were subjected to electrochemical anodization have a combined cylindrical and conical shape with dual thread design, three channels at the apical end of the implant, and a flat cutting apex (fig. 2). Dual thread design enhances the placement procedure, the channels supports self-taping properties and collects bone chips during the insertion, and flat cutting apex allow final adjustments in the course of placement procedure. The implant body and V- thread shape are designed for a smooth insertion process even in compromised bone conditions, offering mild bone compression and maximum initial and long term implant's stability.

Table 1 presents the process parameters used in our experiments and results on morphology and diameters of self-organized oxide nanotubes/nanopores that were synthesized by anodization. The image of the anodized threaded surface of medical implant is shown in figure 2.

The complex shape of the threaded substrates raises challenges in nanostructured oxide layer development regarding multidirectional growth directions, the generation of internal stresses as a result of uneven distribution of the electric field across the surface of the substrate, and of volume expansion during the oxide growth. Nevertheless, a detailed analysis of anodized samples by using SEM images revealed that all the features of threaded surfaces are covered by uniform, ordered nanoporous oxide layer. All anodized implants geometry features (fig. 3a) were investigated: frontal apex, spiral channels, major diameter, minor diameter, and thread flank. SEM micrographs collected at low magnification (1500X) show the oxide layer present on the frontal apex surface (fig. 3b) and spiral channel surface (fig. 3c). The nano-structured

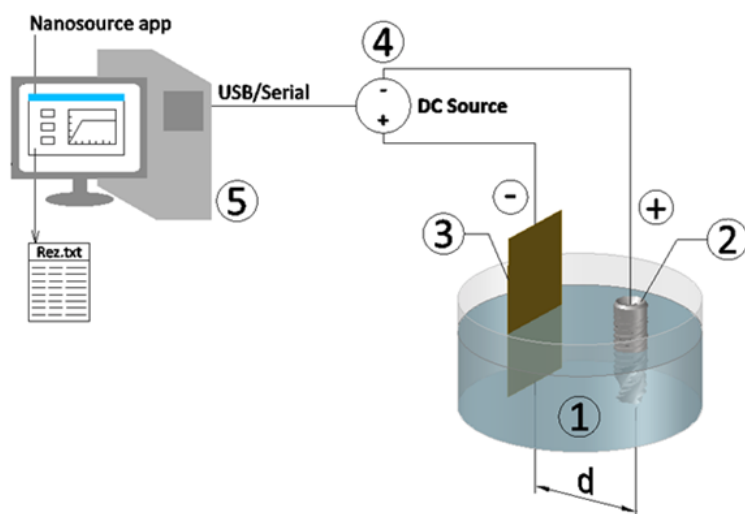


Fig. 1. Electrochemical anodization set-up: 1- electrolyte; 2 -anode - titanium alloy threaded sample (dental implant); 3-cathode - pure copper foil; 4-DC power supply; 5 -originally designed software for process control, visualization and registration of process data (Nanosource 2)

Table 1
ELECTROCHEMICAL ANODIZATION PROCESS PARAMETERS AND RESULTS

Sample designation	Anodization potential U [V]	Current density in potentiostatic stage J [A/m ²]	Morphology of nanostructured oxide layer	Nanostructures internal diameter D _i [nm]	
				min - max [nm]	average [nm]
NS01-THR	24	6.80 - 42.30	nanoporous	24 - 73	40
NS02-THR	30	5.30 - 44.50	nanoporous	24 - 98	63
NS03-PLA	24	19.00 - 45.00	nanotubular	49 - 122	85
NS04-CYL	24	15.00 - 40.00	nanotubular	37 - 98	67

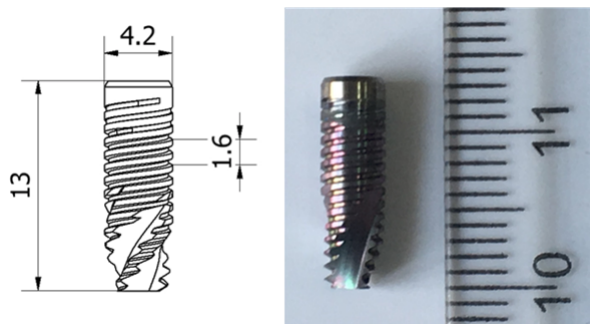


Fig. 2. The blueprint of the implant and the image of the anodized threaded surface of NS-THR01 sample

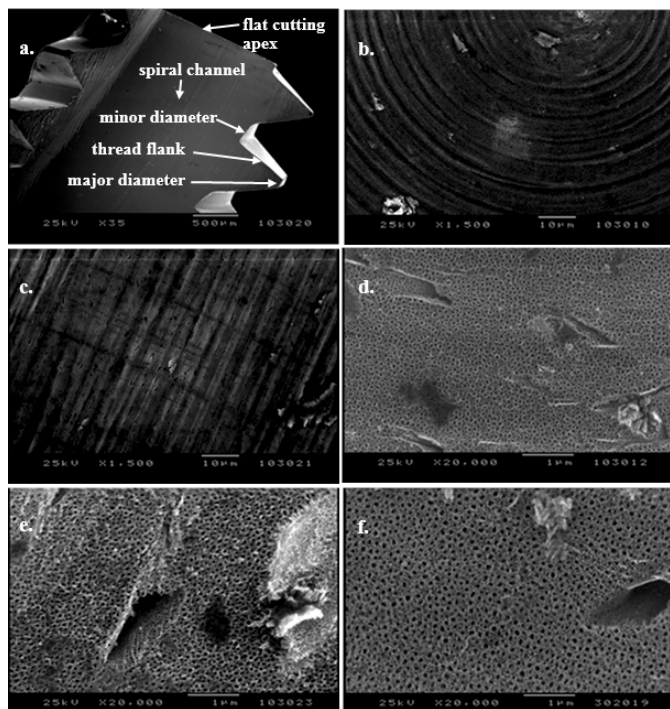


Fig. 3. SEM micrographs of modified threaded surface of Ti6Al4V alloy dental implant subjected to electrochemical anodization in phosphate/fluoride electrolyte; a - implant geometry (35X magnification); b and c - oxide layer on flat cutting apex and on channels at the apical end (1500X); d, e, and f - nanoporous structure of oxide layer on features of threaded surface: d - cutting apex, e - spiral channel, f - minor diameter (20000X)

nature of the oxide layer can be observed at higher magnification (20000X). Figure 3.d presents the nanoporous oxide layer developed on the cutting apex, on figure 3.e one can observe the nanoporous structure on spiral channel, and in figure 3.f the nanopores developed on minor diameter of the implant are shown.

The nanostructures developed on threaded surfaces were compared with the ones developed on planar and cylindrical surfaces synthesized in the same process conditions. The samples NS01-THR, NS03-PLA, and NS04CYL were anodized at anodization potential of 24 V, applied with an initial potential ramp of 0.08 V/S. The SEM analysis shows that on planar and cylindrical surface the oxide layer exhibits nanotubular morphology, with the nanotubes walls clearly split one of each other, while on threaded surface the morphology is a nanoporous one (fig. 4). On planar surface nanotubes have internal diameter of 49-122 nm, the most of them being of ~ 85 nm in diameter (table 1 and fig. 4a). On cylindrical surface the nanotubes are in 37-98 nm diameter range, with an average of 67 nm (table 1 and fig. 4b). As a result of changes in the electrical field lines distribution during the anodization process in the case of cylindrical surface compared to planar surface,

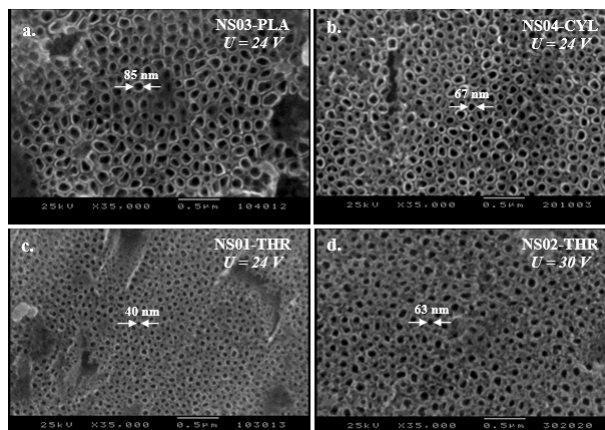


Fig. 4. SEM micrographs of nanostructured surface of Ti6Al4V alloy developed by electrochemical anodization in 1M H_3PO_4 + 0.4 wt.% HF; a - oxide nanotubes developed on planar surface, $U = 24$ V; b - oxide nanotubes developed on cylindrical surface, $U = 24$ V; c - nanoporous oxide developed on threaded surface, $U = 24$ V; d - nanoporous oxide developed on threaded surface, $U = 30$ V (35000X magnification)

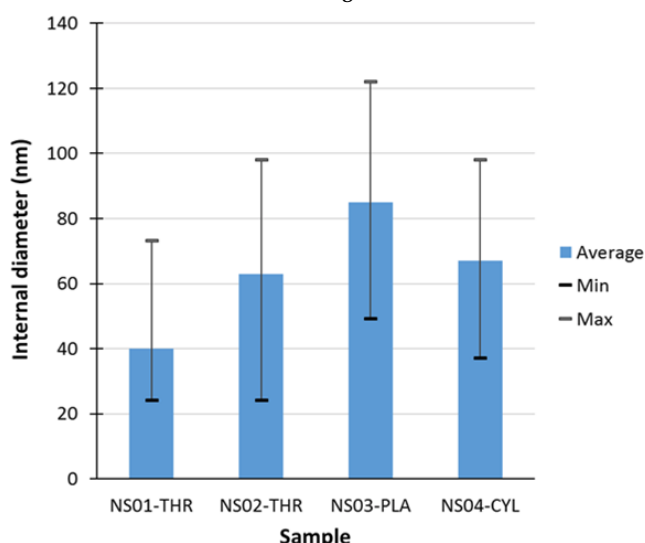


Fig. 5. Internal diameter of electrochemically synthesized nanostructures

the nanotubes diameters suffered a drop of 21% - from 85 nm to 67 nm - taking in account the average values. In the case of complex geometry of threaded surface, anodization led to development of a nanoporous structure, with pore openings in the 24-73 nm, average 40 nm (table 1 and fig. 4c). It is clear that the uneven distribution of electrical field during the anodization affects the nature of the nanostructures that are developing. Even the electrical parameters (anodization potential, potential ramp) are the same, and the current density in the potentiostatic stage of anodization is comparable (table 1), the results on oxide morphology are different. On the threaded surface, due to the uneven distribution of electric field and to difficulties in fluoride ions uptake from electrolyte caused by shielding effect of screw walls, the morphology consists in nanopores, with smaller openings compared to nanotubes developed on planar and cylindrical substrates. Figure 5 reflects these results, showing the decrease of nanostructures diameters on threaded surfaces with 40% compared to cylindrical surfaces (NS01-THR vs. NS04-CYL), and with 53% compared to planar surfaces (NS01-THR vs. NS03-PLA).

In order to enhance the electric field, the sample NS02-THR was developed with an increased anodization potential of 30 V, instead of 24 V. The initial potential ramp was the same, 0.08 V/s. Detailed analysis of numerous

SEM micrographs collected from all surface features of the sample showed the nanostructured oxide layer covering the entire surface of the implant. The morphology of the layer is nanoporous, with pore diameters in 24-98 nm range, average 63 nm. The increasing in nanopores diameter with the increasing in anodization potential can be observed by comparing SEM micrographs collected at a magnification of 35000X from NS01-THR and NS02-THR samples (fig. 4.c and d). In our electrochemical anodization cell, by using as electrolyte a solution of 9.34 wt.% H_3PO_4 + 0.4 wt.% HF, a 25% increase of anodization potential (from 24 V to 30V) led to a 57.5% increase in average nanopores diameters (from 40 nm to 63 nm).

Figure 6 presents the current density evolution during the anodization of threaded samples. The current-time dependence reflects the initial potentiodynamic stage, when the anodization potential was raised from 0 to 24V or 30 V, with a scan of 0.08 V/s. After an initial rapid increase in current density, a steady state occurred, corresponding to the nanopores initiation. After the end potential was reached, the process entered in the potentiostatic stage, where the potential was kept constant. This moment occurred after 300s (5 min) for $U = 24$ V, and after 375s (6min15s) for $U = 30$ V. In this stage, the nanoporous oxide structure continued to grow, the pores deepened inside the substrate surface. Their growth, at the bottom of the oxide layer, requires a certain balance between oxide layer growth at the interface oxide-substrate and the oxide layer dissolution at the interface oxide-electrolyte. This equilibrium is shown by a steady state evolution of current density. In figure 6 appears that this steady state is missing, the current density having a continuous increase during the time of anodization. This is due to the fact that current density was calculated with the initial surface area of the implant that was submerged in the electrolyte (1.324 cm^2) and not with real surface area of the oxide, which can not be accurately calculated for each moment of the anodization process. Having in mind that during the nanoporous oxide growth the actual area of the surface is increasing, it is expected that the plot of current density to present a stable evolution during the potentiostatic stage of anodization.

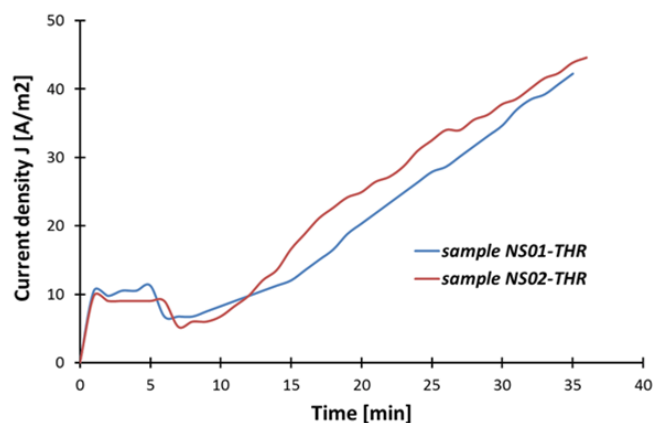


Fig. 6. Current density during electrochemical anodization of Ti6Al4V alloy threaded surfaces

Conclusions

The synthesis of uniform, self arranged nanostructured oxide layer on substrates with complex geometries, made of two phase titanium alloys, with initial micro rough topography, such as many commercial screw-type medical implants are, is a challenging process.

Our results demonstrate the synthesis of continuous nanoporous oxide layers covering all geometrical features (frontal apex, spiral channels, major diameter, minor

diameter, thread flanks) of threaded surfaces. By electrochemical anodization in 9.34 wt.% H_3PO_4 and 0.4 wt.% HF aqueous solution, the morphology of oxide layers consists in nanopores of 24-73 nm diameter (average 40 nm) when using anodization potential of 24V. At increased anodization potential of 30 V, the nanostructured oxide that is developing is also nanoporous, the pores diameters are bigger, being in 24-98 nm range (average 63 nm). The current density during the anodization is below 45 A/m^2 .

Comparing the nanoporous morphology of the oxide layers developed on threaded surfaces ($D_i - 40\text{ nm}$) with the nanotubular morphology that is developing on cylindrical ($D_i - 67\text{ nm}$) or planar surfaces ($D_i - 85\text{ nm}$) our results show that the diameters of nanostructures are smaller on complex geometries, even using the same process parameters for anodization. This is mainly due to the uneven distribution of electrical field and difficulties in fluoride ions (which are essential for nanoporous/nanotubular oxide formation) uptake from electrolyte raised by shielding effect of screw walls. Further research work is planned for optimization of electrochemical anodization in order to synthesize well developed, highly ordered, self arranged nanotubular oxide layers on threaded surfaces of medical implants.

Acknowledgment: This work was supported by a grant of the Romanian National Authority for Scientific Research and Innovation, CNCS/CCCDI-UEFISCDI, project number PN-III-P2-2.1-PED-2016-0142, within PNCDI III.

References

- KULKARNI, M., et al, Nanotechnology, 26, 2015, p. 062002
- KARAZISIS, D., BALLO, A. M., PETRONIS, S., AGHELI, H., EMANUELSSON, L., THOMSEN, P., OMAR, O., Int. J. of Nanomed, 11, 2016, p. 1367
- GULATI, K., MAHER, S., FINDLAY, D., LOSIC, D., Nanomedicine, 11, nr. 14, 2016, p. 1847
- GULATI, K., SASO, I., Expert Opin. Drug Deliv, 14, nr. 8, 2017, p. 1009
- BAENA, R. R., RIZZO, S., MANZO, L., LUPI, S. M., J. Nanomater, 2017, 6092895
- RIBEIRO, A. R., GEMINI-PIPERNI, S., ALVES, S. A., GRANJEIRO, J. M., ROCHA, L.A, Metal Nanoparticles in Pharma, doi.org/10.1007/978-3-319-63790-7_6, 2017, p. 101
- JAGER, M., JENNISSEN, H. P., DITTRICH, F., FISCHER, A., Materials, 10, nr. 11, 2017, p. 1302
- HUANG, Y., et al, Int. J. of Nanomed, 13, 2018, p. 633
- KULKARNI, M., et al, Mater. Sci. Eng. C, 77, 2017, p. 500
- RADTKE, A., et al, Nanomaterials, 7, 2017, p. 197
- ROY, P., BERGER, S., SCHMUKI, P., Angew. Chem. Int., 50, 2011, p. 2904
- DUMITRIU, C., POPESCU, M., VOICU, G., DEMETRESCU, I., Rev. Chim. (Bucharest), 64, no. 6, 2013, p. 600
- KULKARNI, M., MAZARE, A., SCHMUKI, P., IGLIC, A., Advanced Material Letters, 7, nr. 1, 2016, p. 23
- SHAH, U. H., DEEN, K. M., ASGAR, H., RAHMAN, Z., J. Electroanal. Chem., 807, 2017, p. 228
- MENGSHI, Y., et al., Electrochem. Commun., 86, 2018, p. 80
- STOIAN, A. B., et al., Ceram. Int., 44, nr. 6, 2018, p. 7026
- HUIFEI, L., et al., ChemElectroChem, 2018 doi: 10.1002/celec.201701231
- GULATI, K., SANTOS, A., FINDLAY, D., LOSIC, D., J. Phys. Chem. C, 119, 2015, p. 16033
- DING, X., et al, Int. J. Nanomed., 10, 2015, p. 6955
- MONETTA, T., ACQUESTA, A., CARANGELO, A., BELLUCCI, F., Metals, 7, nr. 6, 2017, p. 220
- STRNAD, G., JAKAB-FARKAS, L., CHETAN, P., PETROVAN, C., MATEC Web Conf., 2018, accepted, in press.

Manuscript received: 15.01.2018